AGU ADVANCING EARTH AND SPACE SCIENCES

Water Resources Research

RESEARCH ARTICLE
10.1029/2023WR034910

Key Points:

- We re-evaluate equations proposed by Francis Hall to assess concentration-discharge (*C*-*Q*) relationships using newly available long-term and high-frequency data sets
- Across time steps we find that log-log and log-linear models perform equally well to describe *C*-*Q* relationships
- Parametrization of storage-discharge relationships via recession analyses provides additional insight to *C*-*Q* relationships

Supporting Information:

Supporting Information may be found in the online version of this article.

Correspondence to:

A. S. Wymore,
Adam.Wymore@unh.edu

Citation:

Wymore, A. S., Larsen, W., Kincaid, D. W., Underwood, K. L., Fazekas, H. M., McDowell, W. H., et al. (2023). Revisiting the origins of the power-law analysis for the assessment of concentration-discharge relationships. *Water Resources Research*, *59*, e2023WR034910. https://doi.org/10.1029/2023WR034910

Received 16 MAR 2023
Accepted 14 JUL 2023

Author Contributions:

Conceptualization: Adam S. Wymore, William Larsen, Arial J. Shogren, Shannon L. Speir, Alex J. Webster
Data curation: Hannah M. Fazekas, William H. McDowell, Desneiges S. Murray
Formal analysis: William Larsen, Dustin W. Kincaid, Kristen L. Underwood, Desneiges S. Murray
Funding acquisition: Adam S. Wymore, William H. McDowell
Methodology: Adam S. Wymore, William Larsen, Dustin W. Kincaid, Kristen L. Underwood, Hannah M. Fazekas, Desneiges S. Murray, Arial J. Shogren, Shannon L. Speir, Alex J. Webster
Project Administration: Adam S. Wymore

Revisiting the Origins of the Power-Law Analysis for the Assessment of Concentration-Discharge Relationships

Adam S. Wymore[1], William Larsen[2], Dustin W. Kincaid[3], Kristen L. Underwood[3], Hannah M. Fazekas[1], William H. McDowell[1], Desneiges S. Murray[1], Arial J. Shogren[4], Shannon L. Speir[5], and Alex J. Webster[6]

[1]Department of Natural Resources and the Environment, University of New Hampshire, Durham, NH, USA, [2]Department of Earth, Environmental, and Planetary Sciences, Rice University, Houston, TX, USA, [3]Department of Civil & Environmental Engineering, University of Vermont, Burlington, VT, USA, [4]Department of Biological Sciences, The University of Alabama, Tuscaloosa, AL, USA, [5]Department of Crop, Soil, and Environmental Sciences, University of Arkansas, Fayetteville, AR, USA, [6]Department of Biology, University of New Mexico, Albuquerque, NM, USA

Abstract Concentration-discharge (*C*-*Q*) relationships are frequently used to understand the controls on material export from watersheds. These analyses often use a log-log power-law function ($C = aQ^b$) to determine the relationship between C and Q. Use of the power-law in *C*-*Q* analyses dates to two seminal papers by Francis Hall (1970, https://doi.org/10.1029/WR006i003p00845) and Francis Hall (1971, https://doi.org/10.1029/WR007i003p00591), where he compared six increasingly complex hydrological models, concluding the power-law had the greatest explanatory power. Hall's analyses and conclusions, however, were based on a limited data set, with assumptions regarding water volume and storage, and used simple model selection criteria. While the power-law is applied widely, it has not been rigorously tested and evaluated in over 50 years. We reexamined Hall's original models across time scales using 8 years of high-frequency and weekly specific conductance data and evaluated model performance using more sophisticated model selection criteria. While we found the power-law analysis remains one of the best performing models, other models performed equally as well including the log-linear functional form. Model performance was similar at the sub-daily to weekly scale but varied with sampling method. More complex models performed poorly relative to simpler models and tended to underpredict concentration at flow extremes due to constraints in fitting model parameters to the observed data. While we conclude, based on the data analyzed here, that the power-law remains a suitable model for *C*-*Q* analyses, opportunities exist to refine and differentiate among *C*-*Q* models based on underlying assumptions of data distribution, recession analyses, and for applying models to reactive solutes.

Plain Language Summary Understanding how solute concentrations respond to changes in river flow remains a fundamental challenge in water resources science. Evaluating the relationship between solute concentrations and river flow (or discharge) can provide insight into how watersheds are structured and how they function. Concentration-discharge (*C*-*Q*) relationships can be used to estimate the rate of material export from terrestrial landscapes to surface waters. Many *C*-*Q* analyses use a power-law analysis and model to determine the response of C to variation in Q; yet this model and its embedded assumptions have not been rigorously tested following the development of water quality sensors that provide high-frequency data. Here we revisit eight mathematical models originally developed by Hall (1970, https://doi.org/10.1029/WR006i003p00845) and Hall (1971, https://doi.org/10.1029/WR007i003p00591) that were initially evaluated with only 36 data points. We reexamine Hall's models using eight years of 15-min specific conductivity data and find that while the power-law model still is one of the best models to use in the evaluation of *C*-*Q* relationships. And overall, simpler models outperform more complex models. We discuss many of the assumptions, such as constant load, that underpin *C*-*Q* analyses to demonstrate that future studies could further parameterize *C*-*Q* analyses for more insight on the mechanisms driving solute-discharge relationships.

1. Introduction

Over the last half-century, the relationship between stream water solute concentration and discharge has been documented and interpreted within the hydro-biogeochemical literature (Figure 1). Concentration–discharge (*C*-*Q*) relationships have been quantified across diverse watershed settings, solutes, and spatiotemporal scales. Event-scale *C*-*Q* relationships can be used to identify source pools within watersheds (Rose et al., 2018; Vaughan

Resources: William H. McDowell
Supervision: Adam S. Wymore
Writing – original draft: Adam S. Wymore
Writing – review & editing: Adam S. Wymore, William Larsen, Dustin W. Kincaid, Kristen L. Underwood, Hannah M. Fazekas, William H. McDowell, Desneiges S. Murray, Arial J. Shogren, Shannon L. Speir, Alex J. Webster

et al., 2017) while weekly, seasonal, and annual *C-Q* relationships are commonly used to develop riverine flux estimates (Appling et al., 2015; Aulenbach et al., 2016; Preston et al., 1989). These coarser time scales are also used to characterize typologies of solute generation and transport within and from watersheds (Herndon et al., 2015; Moatar et al., 2017; Zarnetske et al., 2018). Given their relative ease of use and interpretability, *C-Q* patterns are widely applied across disciplines providing an integrative whole-watershed perspective on solute mobilization (Chorover et al., 2017). The advent of high-frequency sensing in concert with enhanced computational power, statistical analyses, and data visualization techniques has deepened the inferences derived from *C-Q* relationships (Fazekas et al., 2020; Hamshaw et al., 2018; Javed et al., 2021; Underwood et al., 2017).

One of the most widely applied *C-Q* analyses is the power-law relationship ($C = aQ^b$), where C and Q are regressed in log-log space, and the parameters a (y-intercept) and b (slope) are derived. The origins of the power-law in *C-Q* analyses can be traced to two seminal papers by Francis Hall (1970, 1971, see also Johnson et al., 1969), with more recent influential papers (e.g., Godsey et al., 2009; Musolff et al., 2015) firmly establishing the power-law model as a standard approach for evaluating *C-Q* relationships. The power-law model has been widely used to describe the hydro-biogeochemical controls on material export, including dissolved organic carbon and nutrients (Fazekas et al., 2020; Speir et al., 2021; Zarnetske et al., 2018), sediments (Underwood et al., 2017), and geogenic ions (Godsey et al., 2009; Wymore et al., 2017). *C-Q* patterns are commonly classified into three primary categories: (a) enrichment or transport limitation where slope $b > 0$; (b) dilution or source limitation where slope $b < 0$; and (c) constant or chemostatic where the power-law slope is at or near zero.

While Hall's models (1970, 1971) provide the basis for our current use of power-law analyses, questions remain about the suitability of the model to describe solute behavior across hydrologic and environmental conditions. Hall's original work developed six increasingly complex mathematical relationships between C and Q (Hall, 1970) and applied them to specific conductance (SpC) data using nine equations (Hall, 1971). Across the six models, Hall made assumptions regarding constituent load, inflow concentration, mixing and control volumes, and storage-discharge relationships. Of the nine equations, Hall concluded the power-law model performed best because of a high coefficient of determination (R^2) while being the most parsimonious model. Hall's conclusions, however, were derived from a small data set ($n = 34$) collected at a weekly or biweekly scale from February to November in a single year. Hall's models also invoked a power-law relationship between catchment storage and discharge (i.e., recession analysis; Brutsaert & Nieber, 1977; Kirchner, 2009), in turn making a simplifying assumption about source water mixing that may not be appropriate for watersheds with complex storage zones and dynamics. A subset of Hall's original models also assumed a chemical mass balance between inflows and pre-existing water storage, a parameter Hall termed C_0. Many of the values used as parameter estimates were derived through a trial-and-error approach rather than empirically. As a result, Hall's evaluation of the utility of the power-law for describing *C-Q* behavior contains limitations and assumptions that have not yet been critically evaluated by leveraging increased data availability.

The analysis of decadal-scale (e.g., weekly grab samples) and novel high-frequency stream water chemistry and discharge data records is challenging the assumption that the power-law is the most appropriate analysis for evaluating *C-Q* relationships (Tunqui Neira et al., 2020, 2021). For example, non-linearities and significant breakpoints in the *C-Q* relationship are often reported (Godsey et al., 2009; Ibarra et al., 2016; Marinos et al., 2020; Moatar et al., 2017; Speir et al., 2021; Underwood et al., 2017; Wymore et al., 2017), and long-term data can yield low coefficients of determination and relatively poor model fits (Minaudo et al., 2019). The evaluation of high-frequency (15-min) solute data has also revealed temporal complexities including *C-Q* relationships that shift among positive and negative slopes and variable goodness-of-fit statistics over time (Fazekas et al., 2020; Zimmer et al., 2019). The evaluation of *C-Q* relationships at different temporal resolutions (e.g., daily vs. long-term composite analyses) leads to misclassifications of watershed *C-Q* behavior and typologies (Fazekas et al., 2020). The increasingly common detection of such complexities raises the question as to whether the power-law remains the most appropriate model for evaluating *C-Q* relationships.

Here, we revisit five of the six conceptual models originally proposed by Hall (1970, 1971) to describe *C-Q* relationships (note that Hall originally proposed six models but eliminated one that he viewed as more suitable for separating two flow components than for modeling *C-Q* relationships). Our objective is to determine whether *C-Q* relationships are still best represented using the power-law equation given our contemporary ability to evaluate *C-Q* relationships across temporal resolutions while leveraging greater computational and statistical power (Fazekas et al., 2020; Javed et al., 2021; Underwood et al., 2017). We ask the following questions: (a) is the

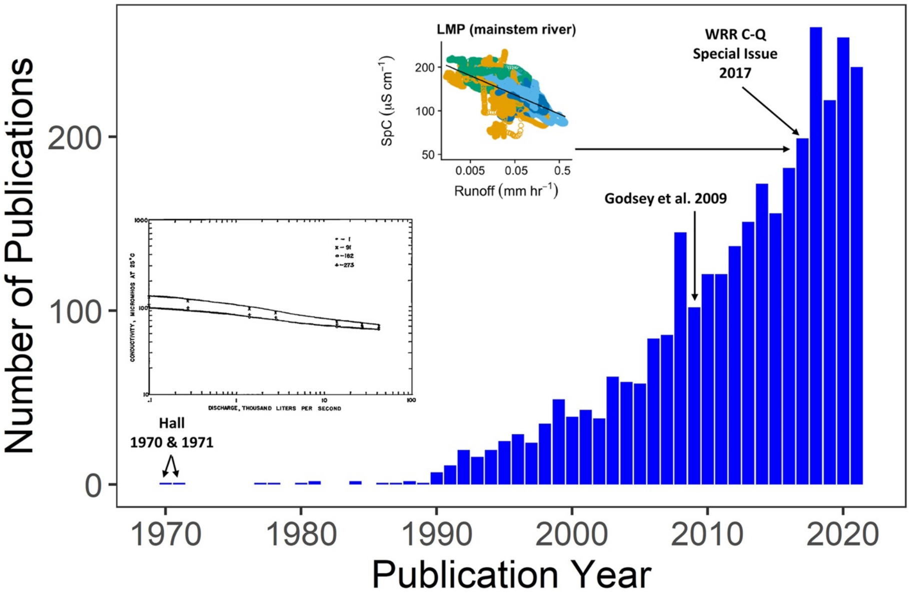

Figure 1. Concentration-discharge (*C-Q*) publications over time (1970–2021). Data are from Web of Science. Highlighted are seminal papers from Hall (1970, 1971), Godsey et al. (2009) and the special issue in Water Resources Research focused on *C-Q* relations in the critical zone. Inset (a) shows Figure 3 from Hall (1971) where the relationship between specific conductance (SpC) and discharge is modeled with six data points. The *y*-axis reads Conductivity, Micromhos at 25°C; the *x*-axis reads Discharge, Thousand Liters per Second. Inset (b) shows the relationship between SpC and runoff derived from a 5-year record of high-frequency data ($n \approx 44{,}000$) from Koenig et al. (2017). Both data sets are from the Lamprey River in New Hampshire (USA).

commonly applied power-law model the best model for describing *C-Q* relationships in increasingly complex long-term and high-frequency data sets? and (b) does the most appropriate model vary depending on the temporal resolution at which *C-Q* relationships are analyzed? To evaluate the original models proposed by Hall, we used both long-term weekly and high-frequency SpC data from the Lamprey River in New Hampshire (USA)—one of the research sites used by Hall in his seminal papers. The high-frequency data allowed us to evaluate model performance across multiple time-steps including the original 15-min record, and downscaled daily, weekly, and monthly time intervals. We also compared model performance at the weekly scale using both lab-analyzed water samples (i.e., weekly grab samples) and values derived from the downscaled sensor data to evaluate whether sampling methodology influenced model performance. We predicted that Hall's power-law model would accurately capture *C-Q* dynamics at longer time steps (e.g., weekly to monthly); however, more complex models would better capture the hydrologic variability controlling *C-Q* relationships at higher resolution time scales (e.g., 15-min).

2. Methods

2.1. Site Description

The Lamprey River is a sixth order river located in southeastern New Hampshire, USA (Figure 2). The Lamprey River has a mean annual discharge of 10,500 L s^{-1} and a median SpC of 146 μS cm^{-1}. Contributions to SpC in the Lamprey River include chemical weathering of bedrock, application of de-icing road salts, and the deposition of sea salt aerosols (Daley et al., 2009; Lazarcik & Dibb, 2017). Land cover is dominated by mixed forests (72%) with the remaining area comprised of wetland (12%), developed areas (6%), and agriculture (3%; NOAA Coastal Change Analysis Program, 2016). Local lithology is comprised of gneiss, granite, metasedimentary and meta volcanic rock with a generally low presence of calcium carbonates. Additional site information can be found in Coble et al. (2018) and Wymore et al. (2021).

2.2. The *C-Q* Data Set

The US Geological Survey (USGS) measures discharge at 15-min intervals (site 01073500, 477 km^2 upstream drainage area; waterdata.usgs.gov). The discharge record includes measurements of flow during reservoir volume

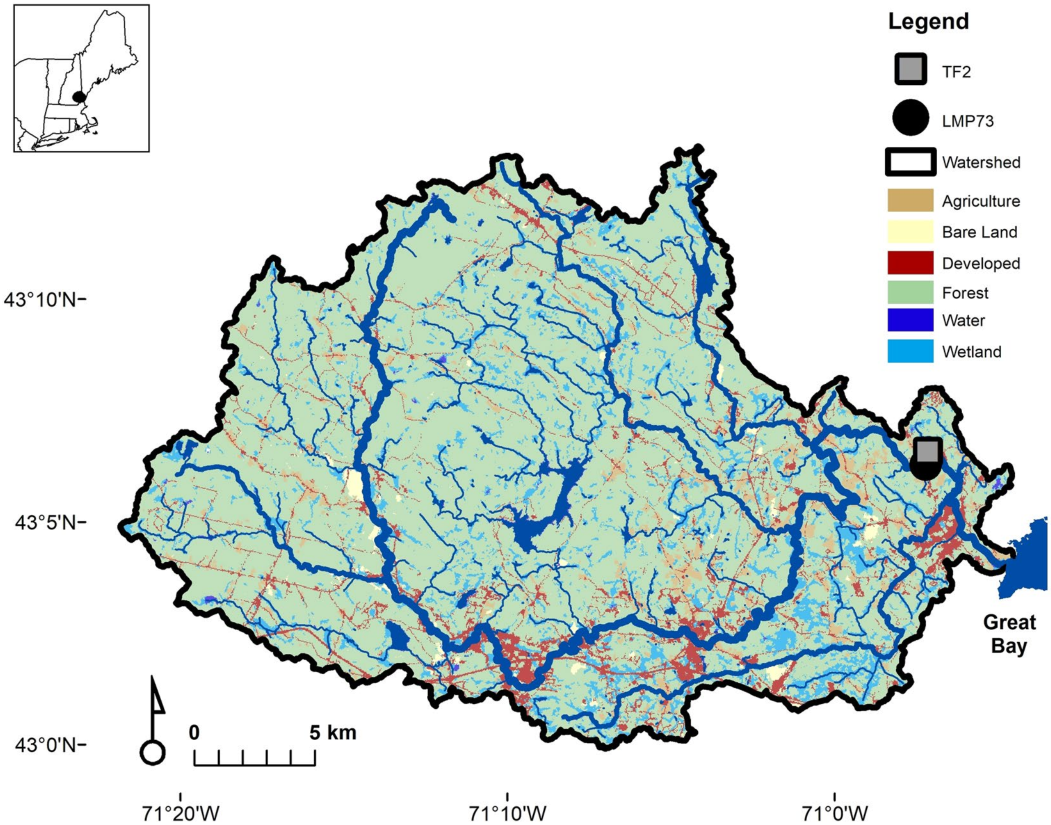

Figure 2. The Lamprey River watershed in southeastern New Hampshire, USA. The Lamprey River mainstem is highlighted with a thick blue line with the sampling site (LMP73) indicated with a black circle and the wet deposition collector (TF2) represented with a gray square. Land-use land-cover data are from NOAA NLCD 2016.

drawdowns. The main reservoir on the Lamprey River is approximately 32 river kilometers above the point of sampling. The reservoir is primarily used for recreation and releases are often in response to the protection of instream flows during periods of low flows. We removed reservoir drawdown events from the discharge and sampling record due to the artificial nature of these flows and their effect on SpC. Across all seasons from 2012 to 2019, SpC was measured weekly using a handheld YSI 556 MPS multi-parameter probe (YSI, Yellow Springs, OH). High-frequency SpC data were collected for the same range of years using an EXO2 multiparameter sonde (YSI, Xylem Inc., Yellow Springs, OH) equipped with hydro-wipers to prevent biofouling during extended deployments. Sensors recorded data at 15-min intervals, and were inspected, cleaned and recalibrated every 6 weeks (see detailed methods in Snyder et al., 2017). We followed standard data quality control practices (Campbell et al., 2013), including drift compensation, comparisons with laboratory-analyzed grab samples, and flagging, omitting, and/or gap-filling data deemed erroneous in the MatLab GCE Toolbox (Sheldon, 2015).

2.3. Model Overview and Parameter Derivation

A note about terminology: Our analysis focuses on five of the six models originally developed by Hall and the eight equations used to examine these models. When describing the methods and results reported here, we primarily use the term equations. We use the term "model fit" to describe the performance of each of the eight equations assessed by model selection criteria described below.

The equations developed by Hall leverage various mathematical techniques. Here, we briefly summarize these equations and explain relevant assumptions and the derivation of two key parameters. The parameter "C_0" represents the concentration of the inflow to the control volume and can represent precipitation, soil water, or both (Godsey et al., 2009; Johnson et al., 1969), but is ultimately sourced from precipitation. The C_0 term is included in equations 2, 5, and 8 (Table 1). The second parameter "n" describes the storage-discharge relationship. All equations incorporate the recession term n. Equations 1–2 take the power-law form; equation 3 uses a log-linear form; equations 4

Table 1
Summary of the Eight Equations Relating to Five Conceptual Models Used to Describe Concentration-Discharge Relationships (After Hall (1970, 1971))

Visualization	Equation		Parameter definition	Model assumptions	Equation # (model # in Hall (1971))
1: Power-law 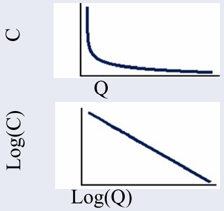	$C = AQ^{-1/n}$	C	Concentration	Single mixing volume, constant load, zero inflow concentration	Equation 1 (Model 1)
		A	Constant (1)		
		Q	Discharge		
		n	Constant exponent		
2: Power-law + C_0 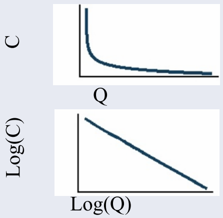	$C = AQ^{-1/n} + C_0$	C	Concentration	Same as 1 with inflow as constant concentration (fixed *y*-intercept)	Equation 2 (Model 2)
		A	Constant (1)		
		Q	Discharge		
		n	Constant exponent		
		C_0	Constant concentration		
3: Log-linear 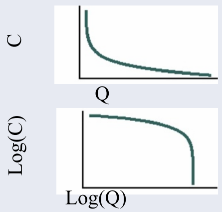	$C = F' - E' \log Q$	C	Concentration	Same as 1 and 2; concentration changes little compared to volume	Equation 3 (Model 3a)
		F'	$F - E * \ln\left(K^{-1/n}\right)$		
		E'	$2.3\frac{E}{n}$		
		Q	Discharge		
4: Stretched exponential 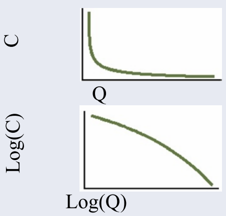	$C = H \exp - G'Q^{-1/n}$	C	Concentration	Same as 1; volume changes little compared to concentration	Equation 4 or 4a (Model 3b)
		H	Constant concentration		
		G'	$\frac{K^{-1/n}}{G}$		
		Q	Discharge		
		n	Constant exponent		
5: Stretched exponential + C_0 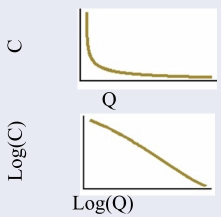	$C = H \exp - G'Q^{-1/n} + C_0$	C	Concentration	Same as 2; volume changes little as compared to concentration	Equation 5 or 5a (Model 3c)
		H	Constant concentration		
		G'	$\frac{K^{-1/n}}{G}$		
		Q	Discharge		
		n	Constant exponent		
		C_0	Constant concentration		

10.1029/2023WR034910

Table 1
Continued

Visualization	Equation		Parameter definition	Model assumptions	Equation # (model # in Hall (1971))
6: Log-linear	$C = M - J'Q^{1/n}$	C	Concentration	Same as 1 or 2; neither volume nor concentration changes much	Equation 6 (Model 3d)
C 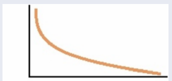 Q		M	Constant concentration		
		J'	$\frac{J * K^{-1/n}}{N}$		
Log(C) 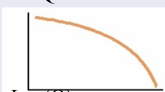 Log(Q)		Q	Discharge		
		n	Constant exponent		
7: Hyperbolic	$C = \frac{S}{1 + BQ^{1/n}}$	C	Concentration	Single mixing volume, inflow = outflow, some part of mixing volume remains constant (V_0). Inflow has no dissolved solids	Equation 7 (Model 4)
C 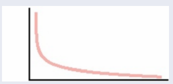 Q		S	Constant concentration		
		B	$K^{-1/n} * V_0^{-1}$		
Log(C) 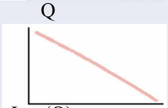 Log(Q)		Q	Discharge		
		n	Constant exponent		
8: Hyperbolic + C_0	$C = \frac{S - C_0}{(1 + BQ^{1/n})} + C_0$	C	Concentration	Single mixing volume, inflow = outflow, some part of mixing volume remains constant (V_0). Inflow has constant concentration (C_0)	Equation 8 (Model 5)
C 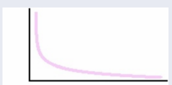 Q		S	Constant concentration		
		C_0	Constant concentration		
		B	$K^{-1/n} * V_0^{-1}$		
Log(C) 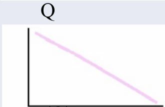 Log(Q)		Q	Discharge		
		n	Constant exponent		
K (constant in $Q = KV^n$)					
n (constant in $Q = KV^n$)					
V (constant in $Q = KV^n$)					
G constant volume					
J constant concentration					

Note. Colors used in the first column are used in subsequent figures to facilitate comparison and tracking of results.

and 5 incorporate a stretched exponential equation, while equations 7 and 8 are described by a hyperbolic function (Table 1). Similar mathematical functions are differentiated by the inclusion of the C_0 term (e.g., equations 1 and 2).

Representing a watershed as a single well-mixed control volume requires several simplifying assumptions (Godsey et al., 2009; Johnson et al., 1969; Seibert et al., 2009). First, the equations evaluated here do not account for any spatial heterogeneity and assume that hillslope and riparian zone characteristics are homogeneous above the point of sampling. Second, it is assumed that precipitation inputs largely infiltrate soils with no preferential flows. Thus, the assumption is that discharged water interacts with unsaturated and saturated soils and reflects a combination of soil water and groundwater that has mixed with and/or been replaced by water added to the control volume. Hall defines this water as inflow (Hall, 1970, 1971), which is represented by the parameter C_0, defined as the solute concentration in the inflow.

The equations outlined by Hall (1970) are centered on a single control volume with some quantity of storage (S) which contributes to river discharge (Q). A power-law relationship between Q and S is prescribed so that $Q = k * S^n$, where k and n are constants. Water in this control volume has a solute concentration (C) and the product of C and total stored water equals the load (L), or total solute mass in the system (where $L = C * S$). Various treatments of the load term enable different representations of the relationship between C and S (e.g., equations 1 and 2 (Table 1) where L is held constant so that $C \propto S^{-1}$). Hydrologic inflows are manifested as changes in S, and a solute C for inflows (C_0) is incorporated by modifying the L equation (e.g., equation 2 (Table 1), $L = (C - C_0) * S$). Equations describing C-S and S-Q relationships are combined by substitution of S, yielding a C-Q relationship.

2.3.1. Concentration of Inflow: The C_0 Term

Three of Hall's equations include a value for the C_0 parameter (Table 1). In Hall's implementation of C_0, SpC was set to either 0 (equations 1, 3, 4, 6, and 7) or within 50–100 µS (µS cm^{-1}) (equations 2, 5, and 8). For these equations, Hall used values that were iteratively estimated by a trial-and-error and linear regression approach and deemed feasible based on the unique geochemistry of the Sleepers River watershed in Vermont, USA (Hall, 1971).

For the Lamprey River, we quantified C_0 based on three sources of conductivity, including wet deposition (i.e., precipitation), soil pore water, and river water at baseflow, which we assumed to be associated with groundwater inputs. We used these values to constrain variability in the inflow concentration. Wet deposition samples were collected weekly year-round from Thompson Farm (43.11°N, 70.95°W) located within the Lamprey River Hydrological Observatory (Murray et al., 2022; Wymore et al., 2021; Figure 2). The Thompson Farm deposition collection site is 23 m above sea level, 20 km from the Atlantic Ocean, and surrounded by mixed deciduous and coniferous forests and agricultural fields (Figure 2). We used a wet-only atmospheric deposition sampler (N-CON Systems Company Inc.; Model 00–120) located on a 30 m walk-up tower. Samples were retrieved approximately every seven days and returned to the University of New Hampshire to be analyzed for SpC using a handheld YSI 556 MPS multi-parameter probe (YSI, Yellow Springs, OH). The mean SpC in wet deposition samples during the study period ($n = 181$) was 9.7 ± 7.8 µS cm^{-1} and was used as the initial C_0 in equations 2, 5, and 8 (Table 1).

We also used two other empirically derived SpC values for C_0 (soil pore water, groundwater) in a sensitivity analysis to understand how model performance responded to variability in inflow concentration (additional details below in Section 2.4.1). Specific conductance from soil pore water was derived from an array of soil sensors located at Thompson Farm that measure electrical conductivity (EC) and temperature at the surface, 15 and 30 cm every 15-min using a Campbell Scientific CS655-L 12 cm Soil Water Content Reflectometers (Campbell Scientific, Logan, UT) and an ECH20 Soil Moisture Sensor 5 TM (Decagon Devices Inc., Pullman, WA, USA). This instrument measures bulk soil EC, but we assume that data are representative of soil pore water which contributes the majority of bulk EC. Soil EC data were trimmed to the same record as the river data and were converted from EC to SpC by SPC = EC/(1 + 0.02 * (Soil Temp − 25°C)). Specific conductance values were averaged across depths and time to derive an integrated C_0 soil value of 591 ± 310 µS cm^{-1}.

As an estimate of the contribution of groundwater to river SpC we used the minimum SpC associated with river baseflow, which we defined as flows with an exceedance probability of 99%. To calculate the exceedance probabilities, we ranked all discharge values from the period of observation for this study. The minimum SpC associated with the 99th flow percentile or greater was ~220 µS cm^{-1}.

2.3.2. Recession Analysis: The "n" Term

Recession analysis is a hydrological modeling technique used to infer changes in watershed storage from measured changes in Q (Brauer et al., 2013; Brutsaert & Nieber, 1977; Jachens et al., 2020; Kirchner, 2009; McMillan

10.1029/2023WR034910

et al., 2014; Sujono et al., 2004). The parameter n included in Hall's equations (Table 1) is derived from Q recession analyses (Hall, 1970, 1971; Snyder, 1969) and describes the nonlinear relationship between Q and S. The recession parameter n can be functionally defined as equal to $\frac{1}{(2-b)}$, where b is the slope of the $-dQ/dt \sim Q$ relationship plotted in log-log space (Kirchner, 2009; Teuling et al., 2010). To mitigate the potential obfuscating effects of precipitation (P) and evapotranspiration (ET), we followed the approach of Kirchner (2009) and used a technique that isolates periods of a Q time series where $Q >> P$, ET (Kirchner, 2009). These criteria constrain our recession analysis in three important ways. First, we assumed that in a humid catchment like the Lamprey River, ET fluxes were minimized at night (Kirchner, 2009); therefore, we excluded periods during the day (5:30 to 19:30). Second, to reduce the influence of P, we excluded Q data points with non-zero P during the previous 12 hr as recorded by a matched hourly P data set (Kirchner, 2009). Hourly P data were obtained from the Climate Reference Network (CRN; GHCND: USW00054795; NH Durham 2 SSW; NOAA National Centers for Environmental Information, 2001). Lastly, to avoid the influence of snowmelt as a delayed P input, we limited the recession analysis to May through October when minimal snowpack was observed at the site. Removing time periods with P or snowmelt also served to limit the analysis to periods when saturation-excess overland flow conditions are minimized and return flow is an insignificant percentage of Q, which is a key assumption of the recession analysis described above (Kirchner, 2009).

We employed a variable time-step approach to determining the parameter n, where dt at time t is incrementally increased, starting at $dt = 1$ hr, until the modified dQ ($dQ = Q(t) - Q(t - \Delta t)$) was greater than 0.001 * mean Q, a threshold meant to approximate the measurement precision of the discharge gage. The resulting dQ/dt value was then paired with mean Q across the same time interval. The central tendency of the recession plot was found by binning the points into ranges of Q that span at least 1% of the logarithmic range in the data set if the standard error of $ln(dQ/dt)$ is less than half the mean dQ/dt in the bin (Kirchner, 2009). The binned data were fit to a power law function $dQ/dt = a * Q^b$ using a linear regression weighted by the inverse of standard errors for each bin, and the slope b is converted to n.

2.4. Model Fitting

We fit the eight C-Q equations (Table 1) to several different SpC and Q data sets from the Lamprey River. We used SpC collected weekly during routine sampling from 2012 to 2019, and 15-min SpC data collected using in-situ sensors during the same 2012–2019 period. We fit each C-Q equation to three additional data sets derived from the 15-min sensor data by downscaling 15-min sensor data to daily, weekly, and monthly frequencies. To derive the downscaled data sets, we randomly selected a specific conductivity measurement at the appropriate frequency using the function "slice_sample" from the "dplyr" package (Wickham et al., 2021; v. 1.0.7) in R (v. 4.1.1). The random samples were limited to measurements made between 8:00 and 16:00 to align with the grab samples collected during daytime hours. For the weekly and monthly data sets, the random samples were further limited to samples measured between Monday and Friday. To assess model fit sensitivity to the random sampling for the downscaled data sets, we derived 10 different iterations of the reduced data sets. We then fit the C-Q models to each data set using nonlinear least squares with the function "nls" in R. To evaluate model performance, we used repeated k-fold cross-validation with 10 folds using the "vfold_cv" function in the "rsample" R package (Silge et al., 2021; v. 0.1.0). We calculated the root mean square error (RMSE) for each model as the standard deviation of the model residuals and used RMSE values to assess model performance where lower values reflect better performing models.

2.4.1. Sensitivity Analysis

We conducted a sensitivity analysis to determine whether the models responded differently to a C_0 derived from wet deposition compared to soil pore water or groundwater inputs. We refit each equation where C_0 was included as a non-zero term (i.e., equations 2, 5, and 8) with the three C_0 values derived from soil pore water and baseflow (Section 2.3.1) using the 15-min sensor data.

3. Results

3.1. Range and Central Tendencies of Lamprey C and Q Data

Grab sample SpC ranged from 39 to 256 μS cm^{-1} with a mean of 145 ± 39 (Figure 3a). High-frequency SpC ranged from 79 to 250 μS cm^{-1} with a mean of 151 ± 34 μS cm^{-1} (Figure 3b). Discharge paired with the grab sample data set ranged from 69 to 79,004 L s^{-1}, while Q paired with the high-frequency data ranged from 60 to 92,313 L s^{-1}. Sampled Q in the Lamprey River ranged across the 4th to 95th percentiles (Figure S1 in Supporting Information S1).

10.1029/2023WR034910

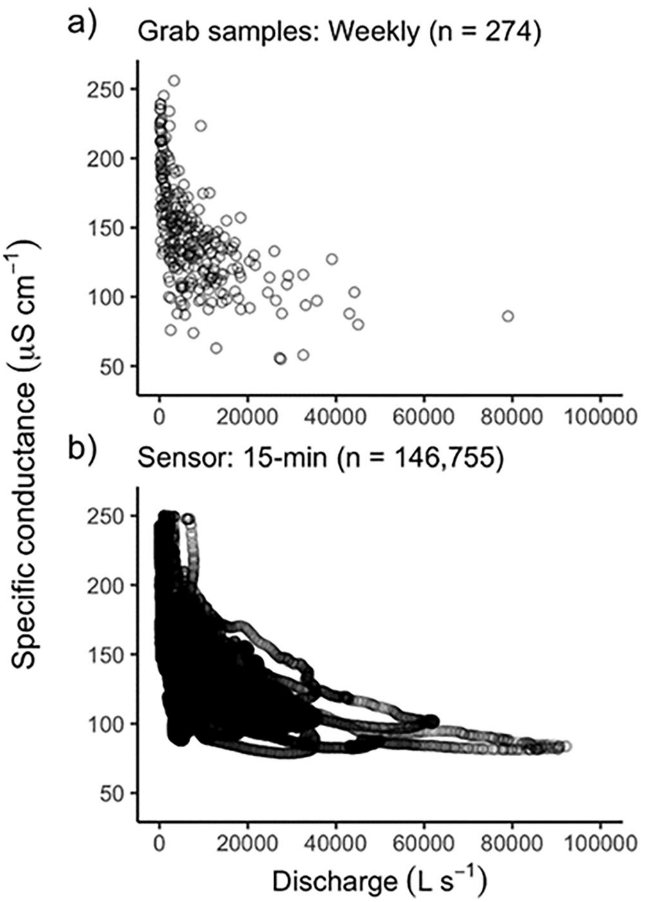

Figure 3. Specific conductance (SpC) and discharge data from the Lamprey River from 2012 to 2019. SpC data were collected (a) weekly as grab samples as part of long-term monitoring or (b) every 15 min with a YSI EXO in situ water quality sensor.

Comparatively, the data set used by Hall (1971) included SpC values that ranged from 110.5 to 317.1 µS cm^{-1} with a mean of 204.0 ± 54.2, and discharge ranged from 66.65 to 9,599 L s^{-1}. Discharges sampled by Hall in the Sleepers Rivers catchment span the 25th to 80th percentiles (Figure S1 in Supporting Information S1).

3.2. *C-Q* Model Performance

We found a general pattern of similar performance among the first three *C-Q* equations (power-law, power-law + C_0, and log-linear; Table 1) at the mid-ranges of measured Q (Figure 4). Equations diverged at the lower and upper ranges of Q (Figure 4). Model fits for equations 1, 2, and 3 were visually indistinguishable, fitting the data better than all other models at the extremes of Q, but displayed variable behaviors of over- and under-predicted C at the upper and lower Q ranges (Figure 4 and see model residuals in Figure S2 in Supporting Information S1). Equations 4–8 all over-predict C at the middle range of Q while under-predicting at both low and high values of Q.

Equations 1–3, which have fewer unknowns and thus did not require the externally derived recession n parameter for fitting, had nearly identical RMSE values (Figure 5). Equations 4 and 5 had similar RMSE values and were consistently higher than equations 7 and 8. RMSE values for equations 4, 5, 7, and 8 were approximately 25% greater than the RMSE values for equations 1–3. Equation 6 had the highest RMSE values of all eight equations.

3.3. Influence of Sample Frequency on *C-Q* Model Performance

Model performance slightly decreased with reduced sampling frequency for the sensor-derived data (Figure 5, Table S1 in Supporting Information S1). Although the differences were minimal, the pattern of increasing RMSE from 15-min to monthly sensor data was consistent across the eight equations. Error surrounding mean RMSE values also increased with downscaled sampling intervals. The full 15-min sensor-derived data set consistently had the lowest RMSE values (Equations 1–3: 20.3–20.7 µS cm^{-1}). Downscaled sensor data to the weekly and monthly time-interval, however, did produce larger confidence intervals around RMSE values, demonstrating that uncertainty surrounding model performance is sensitive to temporal resolution. The greatest difference in model performance occurred between the sensor-derived data sets and the weekly grab sample data set. The RMSEs for equations 1–3 of the weekly grab sample data set (27.1–27.4 µS cm^{-1}) were on average 34% greater than those of equations 1–3 of the full 15-min sensor-derived data set.

3.4. Sensitivity Analysis of C_0

We refit each equation where C_0 was included as a non-zero term (i.e., equations 2, 5, and 8) with the C_0 values derived from wet deposition (9.7 µS cm^{-1}), soil pore water (591 µS cm^{-1}) and baseflow (220 µS cm^{-1}; Section 2.3.1). Mean RMSE values were lowest when using the C_0 associated with wet deposition for all three equations (Figure 6). Using the higher C_0 values increased means RMSE values 68%–69% for equation 2, 10%–16% for equation 5, and 17%–28% for equation 8.

3.5. Recession *n*

The weighted linear regression between log($-dQ/dt$) versus log(Q) for the Lamprey River (Figure 7) produced a recession slope $b = 0.86 \pm 0.01$ which corresponds to a power-law *Q-S* slope of $n = 0.877$. When applied to equations 1 and 2, this result corresponds to a *C-Q* power-law slope $b = -1.14$. However, fitting the *C-Q* data to equations 1 and 2 and solving for n as an unknown yielded much higher n values than from recession analysis. Fitting *C-Q* data using regression for equation 1 yields a b slope of -0.132 corresponding to $n = 7.6$, while equation 2

10.1029/2023WR034910

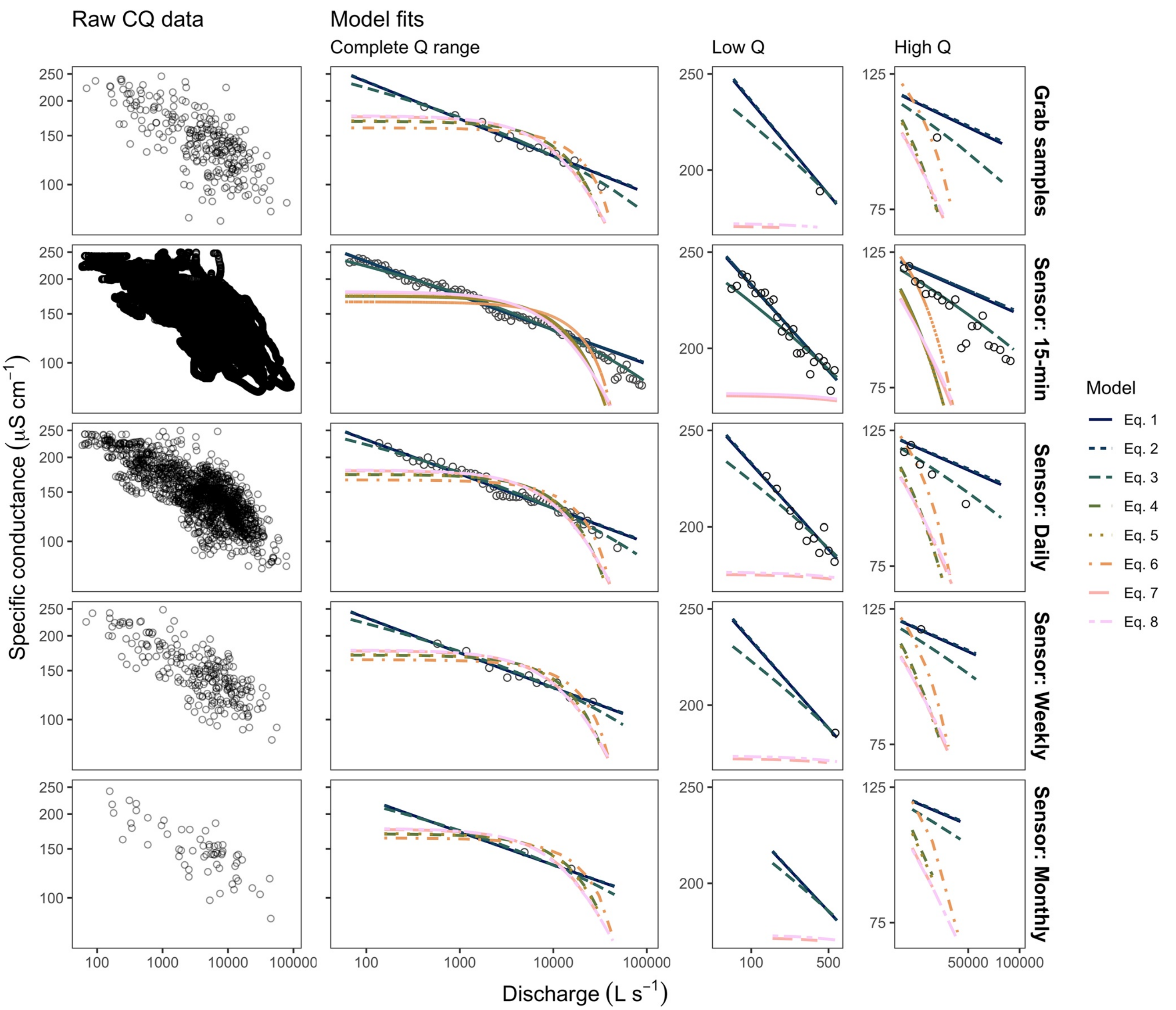

Figure 4. (left) Specific conductance and discharge data from the Lamprey River from 2012 to 2019 used in the nonlinear least squares model fits (right). Axes are $\log_{10}$-transformed. Data sets consisted of all data from the weekly grab sample data set, all 15-min sensor data, and three additional data sets derived from the 15-min sensor data by randomly sampling at daily, weekly, and monthly time scales. Plots on the right display best fit lines for each model equation (Table 1). Open circles overlaid on the best fit lines are raw data binned (Section 2.3.2) to improve visual clarity.

yields a b slope of -0.137 corresponding to $n = 7.31$. All other models contain more than two unknowns including n, and therefore required that n be used as a pre-defined input and not be determined from regression.

4. Discussion

4.1. The Power-Law Model Is Robust, But Discerning Differences Among Models Remains Challenging

The increase in data availability and computational technology did not fundamentally alter our understanding of the appropriateness of the current applications of C-Q analyses and models. To the best of our knowledge, the results reported here represent a much needed rigorous and comparative test of the power-law model to evaluate C-Q relationships and the conclusions presented by Hall. Our analysis addressed several of the limitations to Hall's original approach by increasing sample size by approximately 8,000×, examining model performance across time intervals, and by including data across all four seasons and multiple years. We also applied more robust model selection criteria and a sensitivity analysis to input parameters. We empirically quantified two key

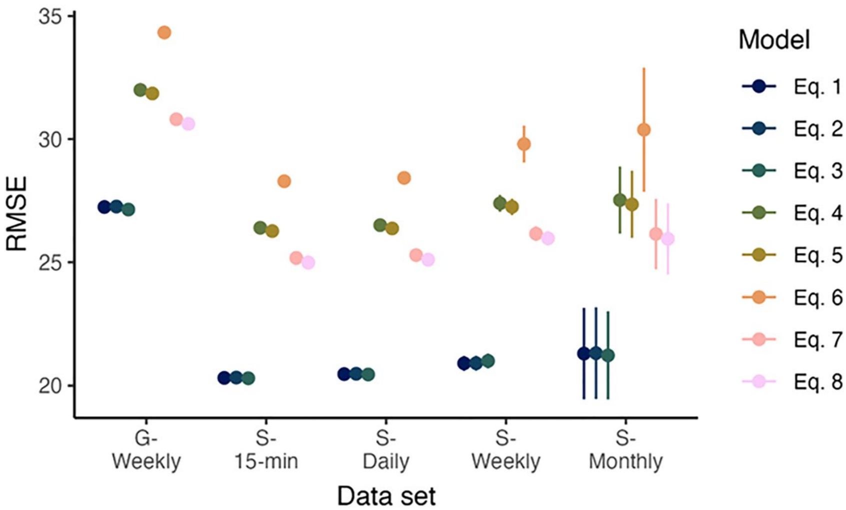

Figure 5. Root mean square error (RMSE) of each nonlinear least squares model fit for each data set (G: grab sample; S: sensor). RMSE were estimated using 10X-repeated 10-fold cross-validation. For data sets derived from the full 15-min sensor data set (S-daily, S-weekly, S-monthly), we repeated the cross-validation for 10 random iterations of the reduced data sets. 95% confidence intervals are plotted but are often obscured by the point size.

parameters, including inflow concentration (C_0) and storage-discharge relationships (n) using site-specific data in contrast to Hall's trial-and-error approach to parameter estimation. Even with this more robust approach, results still support Hall's conclusion that the relatively simple power-law is one of the best performing equations for modeling C-Q relationships. Our results, however, differ from Hall's in that the eight equations separated into two clear groups based on model performance: equations 1–3 and equations 4–8. In Hall's original analysis, these eight equations were nearly indistinguishable based on coefficient of determination with a mean value of 0.908 ± 0.01. In the analysis presented here, the first three equations, which are represented by the power-law, power-law + C_0, and log-linear forms, all perform equally well regardless of sample collection time interval or sampling method—high frequency sensor versus manual grab sample.

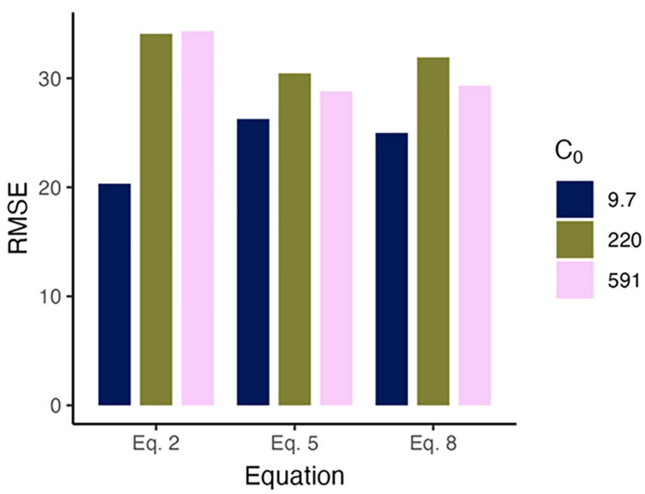

Figure 6. Root mean square error (RMSE) of nonlinear least squares model fit to the 15-min sensor-derived data using the three different C_0 values (9.7 μS cm^{-1}: wet deposition; 220 μS cm^{-1}: baseflow; 591 μS cm^{-1}: soil pore water) for equations where C_0 was included as a non-zero term. RMSE were estimated using 10X-repeated 10-fold cross-validation. 95% confidence intervals are plotted but are too small to be observed at this scale.

Distinguishing model performance between the first three equations may depend on other parameters that covary with Q. The likelihood of other predictors of C is reinforced by the often-reported poor model fits and low coefficients of determination indicating a low percentage of the variability in C is explained by Q (Minaudo et al., 2019). Catchment hydrologic transit time impacts solute concentrations in rivers (Maher & Chamberlain, 2014), and the relationship between transit time and discharge can be highly variable (Torres & Baronas, 2021). It remains unclear, however, whether C is controlled directly by transit time, or whether transit time simply co-varies with another potential causal driver of solute dynamics (e.g., discharge or the mixing of chemically distinct flow paths). The isotopic signature of some solutes (e.g., silica) can be remarkably stable even though transit time distributions and flow pathways can be highly variable (Fernandez et al., 2022). Similar values in Q can also be generated by variable ecohydrological conditions with different corresponding values of C (Bol et al., 2018), which is a defining feature of storm-based data and hysteretic analyses (Evans & Davies, 1998). The mixing of different water and solute sources will also create variability in C. The fractional contribution of different solute reservoirs over time and events of different magnitude and duration will create variability in C (Kurtz et al., 2011). Mixing effects may be especially strong for reactive solutes which vary seasonally due to the phenology of biological processes. The fact that we did not identify one single equation to adequately

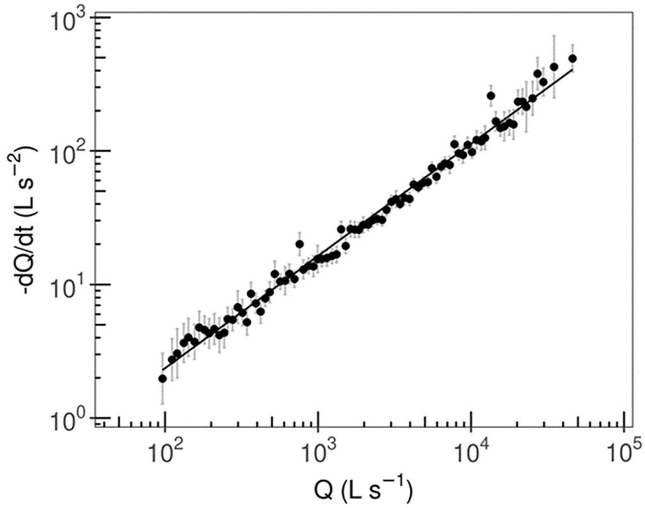

Figure 7. Binned recession plot showing mean values for $-dQ/dt$ and Q using long-term data from Lamprey River USGS station (01073500). Standard errors in gray. Log-log linear regression shown with black line.

represent *C-Q* relationships may be further evidence that *Q* alone is not the best predictor of *C* at the watershed outlet.

Based on the analyses presented here, it is difficult to evaluate when and where these different functional forms (e.g., Equation 1 vs. 3) are most appropriate. Logarithmic transformations are common in the analysis of environmental data and many *C-Q* assessments adopt the power-law and log-log approach without clear statistical justification. While the rationalization for applying the log-log model has a physical basis and interpretation (Godsey et al., 2009), it may underperform in certain situations. For example, in the assessment of multiple base cation *C-Q* relationships from the Hydrological Benchmark Network the power-law did not always provide the best fit (Godsey et al., 2009). Yet, there are relatively few examples of log-linear analyses (i.e., Equation 3) in the *C-Q* literature, although log-linear relationships have been used to predict solute fluxes in montane tropical streams (McDowell & Asbury, 1994) and characterize carbon export regimes across catchments in Patagonia (Perez-Rodriguez & Biester, 2022). The transformation of both concentration and discharge data may not always be appropriate to meet the assumptions of normality given the distribution of the data (McDowell & Asbury, 1994). While it is common for discharge data to vary across multiple orders of magnitude, for many solutes, concentration rarely varies by more than a single factor of ten (e.g., Godsey et al., 2019; Walling, 1975; Wymore et al., 2017). The data set used here aligns with this

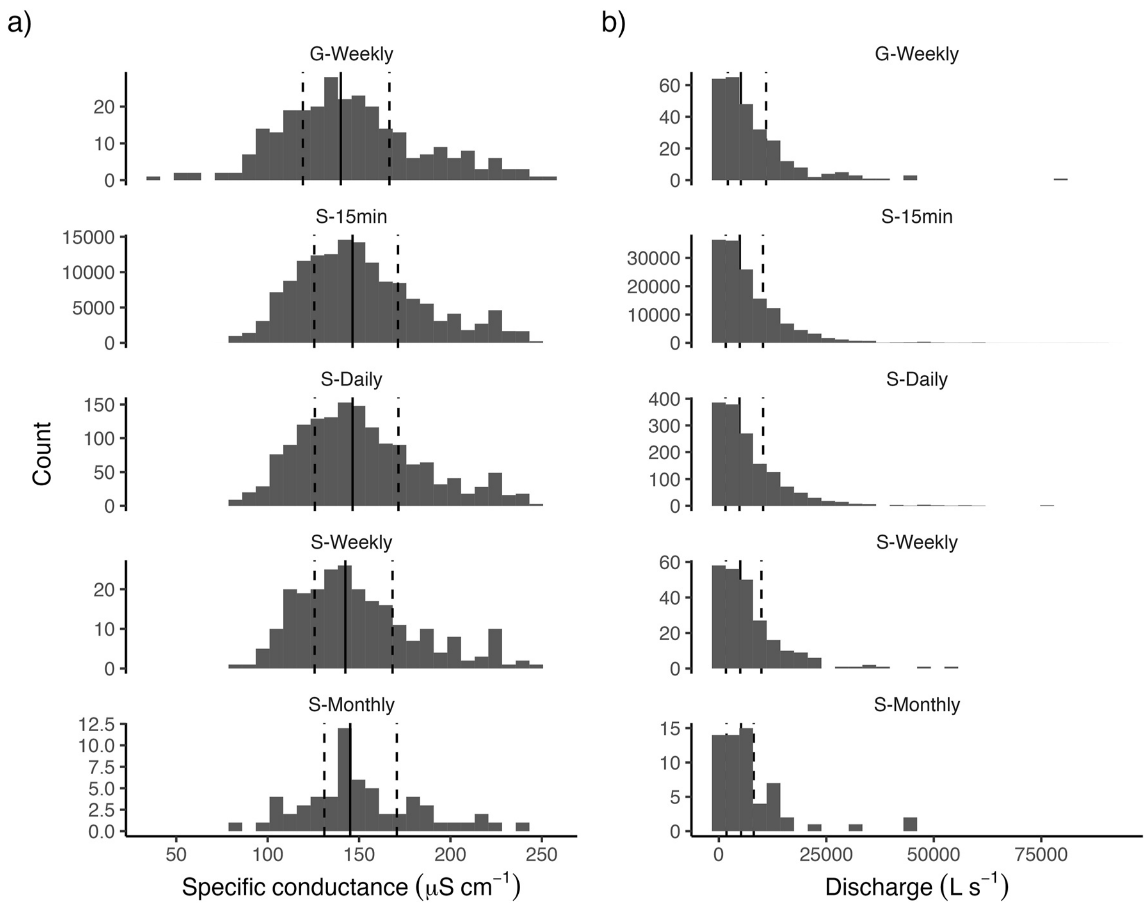

Figure 8. Histograms of (a) concentration and (b) discharge data across the time steps and sampling methods analyzed. Center solid lines represent the median and dashed lines the interquartile range. G is grab sample data and S is sensor data. S-Daily, S-Weekly, and S-Monthly are downscaled data from the S-15-min record.

10.1029/2023WR034910

observation and the assumption of equation 3—that C varies little relative to Q (Figure 8). The log transformation of both variables may be more appropriate in systems that experience large changes in C. For example, in tropical montane systems sediment concentrations and discharge can span similar multiple orders of magnitude (Wymore et al., 2019). A more rigorous test to distinguish the application and performance of the first three equations will require data sets with diverse statistical characteristics and in watersheds where the assumptions underlying the C-Q framework (e.g., mixing dynamics) can be contrasted and tested directly.

The relatively poor performance of models 4–8 is likely the result of underlying assumptions for the various functional forms. In the analyses presented here, the Lamprey River data do not conform to the assumptions of these equations. For example, equations 4 and 5 (stretched exponential) assume that volume changes little compared to C (Table 1). As discussed above, this is an unrealistic assumption for most C-Q data sets and could ultimately constrain the ability of the model to predict well across orders of magnitude of Q. Equation 6 (log-linear), which had the highest RMSE scores, assumes little change in either volume or concentration. While the form of equation 6 shares similarities with the first three equations, the assumption of little variability in both terms likely results in the poor model performance. Lastly, the performance of equations 7 and 8 (hyperbolic) is likely constrained by the assumption that the inflow has no dissolved solids and thus a conductivity of zero. Our empirical analysis of SpC using wet deposition, soil pore water, and baseflow (as a proxy for groundwater), demonstrates a dynamic range of dissolved solid inputs and outputs. The assumptions of equations 7 and 8 are likely not tenable in most watersheds around the world.

Hall attributes his observed model equifinality (although he does not use this phrase specifically) to the use of bulk measurements, such as total dissolved solids and EC (Hall, 1971). Bulk measurements of surface water chemistry likely contribute to model equifinality because they serve as proxies for concentration of multiple solutes simultaneously. This may even influence the results reported here for equations 1–3. Hall writes, "*An examination of other chemical data, if available, along with knowledge of the stream help [sic] decide which model is most suitable*" (Hall, 1971). Model convergence may then be driven by variable responses to flow among the different solutes characterized by SpC. For example, chloride, which contributes to SpC in the Lamprey River (Daley et al., 2009), is usually expected to dilute with increases in discharge (e.g., Hunsaker & Johnson, 2017; Rose et al., 2018). However, there are times of year within the Lamprey River where chloride concentrations increase with flow (Shattuck et al., 2023). Testing for variability among solutes that contribute to SpC as well as characterizing intra-annual and seasonal patterns of specific ions is key to understanding mechanisms behind model equifinality and for improved model performance.

We also observed differences in RMSE values between downscaled sensor data at the weekly scale and weekly grab sample data. It is not entirely clear why this difference in model performance exists. While the distribution of the data is very similar, there is a slight difference in the central tendency between the two data records with mean SpC slightly lower than downscaled weekly data from the sensor record (Figure 8). Notably, sensor locations can be slightly different than where grab samples are collected or grab samples may be collected consistently at certain times of day. Different locations in the channel or times of day may result in different hydro-chemical and metabolic dynamics that drive variability in the concentration and stoichiometry of those solutes that contribute to SpC. This could ultimately be expressed in reduced model performance of weekly grab sample data. While we were able to confirm that no diel patterns were impacting the grab sample data set, and our downscaled data sets contained no such differences to the raw sensor data, variability of sampling location and timing may impact low frequency data sets and ultimately model performance in other cases.

4.2. Assumptions of *C*-*Q* Models and the Recession Term

Broadly, C-Q analyses, and the use of linear models, contain many assumptions that likely impact model performance. These assumptions, which are inconsistently addressed in the literature, include, for example, the homogeneity of landscape characteristics above the point of sampling, a well-mixed control volume and no preferential flows, and constant load. For instance, the assumption of no preferential flow may be tenuous in many watersheds. Flow heterogeneity, which is a function of variability in landscape and subsurface properties (McDonnell et al., 2007), has direct consequences for solute leaching (Radolinski et al., 2022; Šimůnek et al., 2003). The assumption of a constant load which underlies seven of the eight equations evaluated here (all but Equation 8), requires that C is inversely proportional to storage (S). For a linear reservoir, where Q is negatively correlated with S (e.g., equations 1 and 2), simple dilution should result in an inverse relationship between C and Q, or a

10.1029/2023WR034910

power-law slope $b = -1$. Simple dilution of a linear reservoir is frequently presented as a null hypothesis which is rejected if an observed *C*-*Q* slope is greater than -1 (e.g., Godsey et al., 2009; Wymore et al., 2017). A non-linear reservoir, however, embeds a different Q-S relationship where Q is inversely proportional to S^n so that C relates negatively to $Q^{-1/n}$. In this relationship, increasing the recession n drives the apparent *C*-*Q* power law b slope toward zero. The hypothetical case of simple dilution may therefore exhibit a wide variety of apparent *C*-*Q* slopes, depending on the non-linearity of the Q-S relationship.

To the extent that catchments can be represented as simple systems where outflow depends only on storage, computing the recession n may complement *C*-*Q* analysis. In the case of the Lamprey River, $n = 0.877$ so that simple dilution predicts a power-law *C*-*Q* slope $b = -1.1$. The *C*-*Q* data display a slope $b = -0.13$, which demonstrates that simple dilution alone cannot explain the solute dynamics of the Lamprey River. Rather, if simple dilution were to explain *C*-*Q* relationships at the Lamprey River, a recession n of 7.7 would be necessary. Such an elevated value for n implies a pronounced response of Q for small changes in S, and the Lamprey River does not exhibit this behavior. However, a wide variety of recession behavior is observed in other watersheds throughout the continental United States, depending heavily on the technique used to carry out recession analysis (Tashie et al., 2020). It is therefore plausible that a wide variety of *C*-*Q* slopes could be generated for the hypothetical case of simple dilution. The recession slope n is a critical parameter of some *C*-*Q* models (see Appendix of Godsey et al., 2009), and this study emphasizes that recession analysis is a necessary consideration when evaluating controls on *C*-*Q* relationships.

Following Hall, we incorporated the n parameter to account for Q-S relationships. While we empirically determined n for the Lamprey River, and Hall used trial and error, both assessments used a single input value. However, catchment processes that are amplified or suppressed at different intervals of discharge, or at certain times of year, may create variability in the slope of the Q-S relationship. Incorporating variability from the Q-S relationship may increase model sensitivity to the recession n parameter. The evaluated equations all assume an unchanging mixing volume, and the quantification of bank-full discharges may explain why the simpler equations (e.g., equations 1 and (b) tended to overpredict specific conductivity at the highest flows especially at more coarse time intervals. While we intended to keep our analysis similar to Hall in certain ways, a post-hoc analysis of the Lamprey River recession curve (Figure 6) reveals a significant breakpoint at a discharge of 21,300 L/s, which equates to approximately a 1-year return interval based on flow-frequency analysis performed on an 87-year record (1935–2021) of USGS stream flow in the Lamprey River (Figure S3 in Supporting Information S1). A statistically different slope above this inflection point translates to a new n parameter. Allowing for non-linear dynamics in the recession analysis may account for various catchment processes each with unique time constraints that do not conform to the assumptions of linearity (Buytaert et al., 2004), especially at the extreme ends of the flow distribution where most equations tended to underpredict concentration. The identified breakpoint in the Lamprey River likely represents bank-full discharges (Figure S3 in Supporting Information S1), and the expected expansion of flows into the floodplain may be engaging the numerous proximal wetlands that exist along the Lamprey River network. Expansion into floodplain wetlands can introduce new water depleted in specific conductivity (Johnston et al., 1990). This example of bank-full discharges and floodplain interaction exemplifies Hall's point for the need of site-specific knowledge (Hall, 1971). Identifying meaningful breakpoints in discharge via recession analysis provides site-specific criteria for the evaluation of *C*-*Q* relationships above and below critical thresholds.

4.3. New Opportunities to Understand Drivers of *C*-*Q* Relationships

The power-law model is widely used in the analysis of *C*-*Q* relationships, especially following the seminal "chemostasis" paper by Godsey et al. (2009), and our results confirm its utility. Other key questions remain, however, regarding the statistical robustness and explanatory power of the power-law analysis. While commonly applied throughout the literature, a statistical evaluation of the regression relationship that describes the dependency of C on Q is rarely performed, such that the *C*-*Q* power-law correlation is not usually compared to a null model. Data with strong autocorrelative characteristics, such as C and Q data, can artificially inflate explanatory power and type-1 error (i.e., false positive). Given the increasing availability of high-frequency data sets, traditional statistical evaluations of linear regression models may be limited because statistical significance (i.e., *p*-values) can be attributed simply to large sample sizes despite effect size of the predictor variable remaining small (Head et al., 2015; Khalilzadeh & Tasci, 2017). While beyond the scope of our study, approaches such as Monte Carlo simulations, Bayesian linear regression methods (Underwood et al., 2017), and/or time series analysis would be valuable to incorporate into standard use of the power-law model to establish whether or not a *C-Q* relationship is in fact different from a random model (i.e., correlation value or regression slope credibly different from zero).

Our model results and observations open new opportunities to explore the utility of other forms of *C-Q* analysis, raising questions of when and where different functional forms should be applied. We urge future studies of watershed export behavior to incorporate comparative *C-Q* analyses to garner additional insights on model performance across diverse settings. For example, model evaluation of a single or multiple solute type(s) (e.g., conservative geogenic solutes or reactive nutrients) across biomes, basins of various sizes, and landscapes with highly modified hydrology (e.g., urban or tile-drained agricultural streams) could provide additional guidance on model performance and application. The determination of best fit models has many practical implications including for the estimation of solute fluxes where parameters from the *C-Q* relationship are considered central pieces of information (Aulenbach et al., 2016; Preston et al., 1989). The body of literature using *C-Q* relationships to explore the controls on material export from watersheds has been working under multiple assumptions that are rarely acknowledged, including those regarding data transformations, constant load, a single mixing volume, and consistent and linear Q-S relationships. The assumption of constant load may not hold for solutes that have a strong biological signature such as dissolved organic carbon, which rarely shows dilution behavior (Zarnetske et al., 2018). Solutes with strong seasonality also likely violate the assumption of constant load. Assumptions no doubt aid in balancing interpretation versus model complexity. Evaluating Hall's eight equations in the context of other solutes, and at sites with a highly characterized hydrological and critical zone architecture, may provide valuable insight into when and where we can apply the different forms of *C-Q* relationships developed by Hall nearly 50 years ago.

Conflict of Interest

The authors declare no conflicts of interest relevant to this study.

Data Availability Statement

The long-term and grab sample data associated with this study are available through the Environmental Data Initiative and posted at the following resource available in the public domain: https://portal.edirepository.org/nis/mapbrowse?scope=edi&identifier=901&revision=1. The high frequency sensor data are posted on CUAHSI Hydroshare at the following resources available in the public domain: http://www.hydroshare.org/resource/8217eab0997d493782ff321ca5f95f28 (Potter et al., 2020).

Acknowledgments
The authors thank the Water Quality Analysis Lab at the University of New Hampshire including Jody Potter, Michelle Shattuck, and Lisle Snyder. Funding was provided by the National Science Foundation (NSF) and EPSCoR projects Canary in the Watershed (NSF EPS-1929148; ASW) and Ecosystems and Society (NSF EPS-1101245; WHM). Support was also provided by the NSF-funded Belmont Forum project ABRESO (NSF-2129383). Partial funding was provided by the New Hampshire Agricultural Experiment Station. This work was supported by the USDA National Institute of Food and Agriculture Hatch Multi-State Project 1022291 (ASW) and McIntire-Stennis Project 1019522 (WHM). This is scientific contribution 2968. DWK and KLU acknowledge funding from NSF EAR-2012123 and NSF EAR-2033995. Support for DSM was provided by the NASA FINESST program (Grant 80NSSC1441). The authors thank the *C-Q* Network, Christina Richardson, and Joanna Blaszczak for additional discussion and assistance with Figure 1: of *C-Q* publications over time. The authors also thank two reviewers for their helpful comments and insights which improved the manuscript.

References

Appling, A. P., Leon, M. C., & McDowell, W. H. (2015). Reducing bias and quantifying uncertainty in watershed flux estimates: The R package loadflex. *Ecosphere*, *6*(12), 225–269. https://doi.org/10.1890/ES14-00517.1

Aulenbach, B. T., Burns, D. A., Shanley, J. B., Yanai, R. D., Bae, K., Wild, A. D., et al. (2016). Approaches to stream solute load estimation for solutes with varying dynamics from five diverse small watersheds. *Ecosphere*, *7*(6). https://doi.org/10.1002/ecs2.1298

Bol, R., Gruau, G., Mellander, P. E., Dupas, R., Bechmann, M., Skarbøvik, E., et al. (2018). Challenges of reducing phosphorus based water eutrophication in the agricultural landscapes of Northwest Europe. *Frontiers in Marine Science*, *5*. https://doi.org/10.3389/fmars.2018.00276

Brauer, C. C., Teuling, A. J., Torfs, P. J., & Uijlenhoet, R. (2013). Investigating storage-discharge relations in a lowland catchment using hydrograph fitting, recession analysis, and soil moisture data. *Water Resources Research*, *49*(7), 4257–4264. https://doi.org/10.1002/wrcr.20320

Brutsaert, W., & Nieber, J. L. (1977). Regionalized drought flow hydrographs from a mature glaciated plateau. *Water Resources Research*, *13*(3), 637–643. https://doi.org/10.1029/WR013i003p00637

Buytaert, W., De Bièvre, B., Wyseure, G., & Deckers, J. (2004). The use of the linear reservoir concept to quantify the impact of changes in land use on the hydrology of catchments in the Andes. *Hydrology and Earth System Sciences*, *8*(1), 108–114. https://doi.org/10.5194/hess-8-108-2004

Campbell, J. L., Rustad, L. E., Porter, J. H., Taylor, J. R., Dereszynski, E. W., Shanley, J. B., et al. (2013). Quantity is nothing without quality: Automated QA/QC for streaming environmental sensor data. *BioScience*, *63*(7), 574–585. https://doi.org/10.1525/bio.2013.63.7.10

Chorover, J., Derry, L. A., & McDowell, W. H. (2017). Concentration-discharge relations in the critical zone: Implications for resolving critical zone structure, function, and evolution. *Water Resources Research*, *53*(11), 8654–8659. https://doi.org/10.1002/2017WR021111

Coble, A. A., Wymore, A. S., Shattuck, M. D., Potter, J. D., & McDowell, W. H. (2018). Long-term trends in solute concentrations and fluxes from a suburban watershed: Evaluating effects of 100-year flood events. *Journal of Geophysical Research: Biogeosciences*, *123*(9), 3072–3087. https://doi.org/10.1029/2018JG004657

Daley, M. L., Potter, J. D., & McDowell, W. H. (2009). Salinization of urbanizing New Hampshire streams and groundwater: Effects of road salt and hydrologic variability. *Journal of the North American Benthological Society*, *28*(4), 929–940. https://doi.org/10.1899/09-052.1

Evans, C., & Davies, T. D. (1998). Causes of concentration/discharge hysteresis and its potential as a tool for analysis of episode hydrochemistry. *Water Resources Research*, *34*(1), 129–137. https://doi.org/10.1029/97wr01881

Fazekas, H. M., Wymore, A. S., & McDowell, W. H. (2020). Dissolved organic carbon and nitrate concentration-discharge behavior across scales: Land use, excursions, and misclassification. *Water Resources Research*, *56*(8). https://doi.org/10.1029/2019WR027028

Fernandez, N. M., Bouchez, J., Derry, L. A., Chorover, J., Gaillardet, J., Giesbrecht, I., et al. (2022). Resiliency of silica export signatures when low order streams are subject to storm events. *Journal of Geophysical Research: Biogeosciences*, *127*(5), e2021JG006660. https://doi.org/10.1029/2021JG006660

Godsey, S. E., Hartmann, J., & Kirchner, J. W. (2019). Catchment chemostasis revisited: Water quality responds differently to variations in weather and climate. *Hydrological Processes*, *33*(24), 3056–3069. https://doi.org/10.1002/hyp.13554

Godsey, S. E., Kirchner, J. W., & Clow, D. W. (2009). Concentration–discharge relationships reflect chemostatic characteristics of US catchments. *Hydrological Processes*, *23*(13), 1844–1864. https://doi.org/10.1002/hyp.7315

Hall, F. R. (1970). Dissolved solids-discharge relationships: 1. Mixing models. *Water Resources Research*, *6*(3), 845–850. https://doi.org/10.1029/WR006i003p00845

Hall, F. R. (1971). Dissolved solids-discharge relationships: 2. Applications to field data. *Water Resources Research*, *7*(3), 591–601. https://doi.org/10.1029/WR007i003p00591

Hamshaw, S. D., Dewoolkar, M. M., Schroth, A. W., Wemple, B. C., & Rizzo, D. M. (2018). A new machine-learning approach for classifying hysteresis in suspended-sediment discharge relationships using high-frequency monitoring data. *Water Resources Research*, *54*(6), 4040–4058. https://doi.org/10.1029/2017WR022238

Head, M. L., Holman, L., Lanfear, R., Kahn, A. T., & Jennions, M. D. (2015). The extent and consequences of p-hacking in science. *PLoS Biology*, *13*(3), e1002106. https://doi.org/10.1371/journal.pbio.1002106

Herndon, E. M., Dere, A. L. D., Sullivan, P. L., Norris, D., Reynolds, B., & Brantley, S. L. (2015). Landscape heterogeneity drives contrasting concentration-discharge relationships in shale headwater catchments. *Hydrology and Earth System Sciences*, *19*(8), 3333–3347. https://doi.org/10.5194/hess-19-3333-2015

Hunsaker, C. T., & Johnson, D. W. (2017). Concentration-discharge relationships in headwater streams of the Sierra Nevada, California. *Water Resources Research*, *53*(9), 7869–7884. https://doi.org/10.1002/2016wr019693

Ibarra, D. E., Caves, J. K., Moon, S., Thomas, D. L., Hartmann, J., Chamberlain, C. P., & Maher, K. (2016). Differential weathering of basaltic and granitic catchments from concentration-discharge relationships. *Geochimica et Cosmochimica Acta*, *190*, 265–293. https://doi.org/10.1016/j.gca.2016.07.006

Jachens, E. R., Rupp, D. E., Roques, C., & Selker, J. S. (2020). Recession analysis revisited: Impacts of climate on parameter estimation. *Hydrology and Earth System Sciences*, *24*(3), 1159–1170. https://doi.org/10.5194/hess-24-1159-2020

Javed, A., Hamshaw, S. D., Lee, B. S., & Rizzo, D. M. (2021). Multivariate event time series analysis using hydrological and suspended sediment data. *Journal of Hydrology*, *593*, 125802. https://doi.org/10.1016/j.jhydrol.2020.125802

Johnson, C. A., Detenbeck, N. E., & Niemi, G. J. (1990). The cumulative effect of wetlands on stream water quality and quantity. A landscape approach. *Biogeochemistry*, *10*, 105–141. https://doi.org/10.1007/BF00002226

Johnson, N. M., Likens, G. E., Bormann, F. H., Fisher, D. W., & Pierce, R. S. (1969). A working model for the variation in stream water chemistry at the Hubbard Brook Experimental Forest, New Hampshire. *Water Resources Research*, *5*(6), 1353–1363. https://doi.org/10.1029/WR005i006p01353

Khalilzadeh, J., & Tasci, A. D. (2017). Large sample size, significance level, and the effect size: Solutions to perils of using big data for academic research. *Tourism Management*, *62*, 89–96. https://doi.org/10.1016/j.tourman.2017.03.026

Kirchner, J. W. (2009). Catchments as simple dynamical systems: Catchment characterization, rainfall-runoff modeling, and doing hydrology backward. *Water Resources Research*, *45*(2). https://doi.org/10.1029/2008WR006912

Koenig, L. E., Shattuck, M. D., Snyder, L. E., Potter, J. D., & McDowell, W. H. (2017). Deconstructing the effects of flow on DOC, nitrate, and major ion interactions using a high-frequency aquatic sensor network. *Water Resources Research*, *53*(12), 10655–10673. https://doi.org/10.1002/2017WR020739

Kurtz, A. C., Lugolobi, F., & Salvucci, G. (2011). Germanium-silicon as a flow path tracer: Application to the Rio Icacos watershed. *Water Resources Research*, *47*(6). https://doi.org/10.1029/2010WR009853

Lazarcik, J., & Dibb, J. E. (2017). Evidence of road salt in New Hampshire's snowpack hundreds of meters from roadways. *Geosciences*, *7*(3), 54. https://doi.org/10.3390/geosciences7030054

Maher, K., & Chamberlain, C. P. (2014). Hydrologic regulation of chemical weathering and the geologic carbon cycle. *Science*, *343*(6178), 1502–1504. https://doi.org/10.1126/science.1250770

Marinos, R. E., Van Meter, K. J., & Basu, N. B. (2020). Is the river a chemostat? Scale versus land use controls on nitrate concentration-discharge dynamics in the upper Mississippi river basin. *Geophysical Research Letters*, *47*(16), e2020GL087051. https://doi.org/10.1029/2020GL087051

McDonnell, J. J., Sivapalan, M., Vaché, K., Dunn, S., Grant, G., Haggerty, R., et al. (2007). Moving beyond heterogeneity and process complexity: A new vision for watershed hydrology. *Water Resources Research*, *43*(7). https://doi.org/10.1029/2006WR005467

McDowell, W. H., & Asbury, C. E. (1994). Export of carbon, nitrogen, and major ions from three tropical montane watersheds. *Limnology & Oceanography*, *39*(1), 111–125. https://doi.org/10.4319/lo.1994.39.1.0111

McMillan, H., Gueguen, M., Grimon, E., Woods, R., Clark, M., & Rupp, D. E. (2014). Spatial variability of hydrological processes and model structure diagnostics in a 50 km^2 catchment. *Hydrological Processes*, *28*(18), 4896–4913. https://doi.org/10.1002/hyp.9988

Minaudo, C., Dupas, R., Gascuel-Odoux, C., Roubeix, V., Danis, P. A., & Moatar, F. (2019). Seasonal and event-based concentration-discharge relationships to identify catchment controls on nutrient export regimes. *Advances in Water Resources*, *131*, 103379. https://doi.org/10.1016/j.advwatres.2019.103379

Moatar, F., Abbott, B. W., Minaudo, C., Curie, F., & Pinay, G. (2017). Elemental properties, hydrology, and biology interact to shape concentration-discharge curves for carbon, nutrients, sediment, and major ions. *Water Resources Research*, *53*(2), 1270–1287. https://doi.org/10.1002/2016WR019635

Murray, D. S., Shattuck, M. D., McDowell, W. H., & Wymore, A. S. (2022). Nitrogen wet deposition stoichiometry: The role of organic nitrogen, seasonality, and snow. *Biogeochemistry*, *160*(3), 301–314. https://doi.org/10.1007/s10533-022-00966-0

Musolff, A., Schmidt, C., Selle, B., & Fleckenstein, J. H. (2015). Catchment controls on solute export. *Advances in Water Resources*, *86*, 133–146. https://doi.org/10.1016/j.advwatres.2015.09.026

NOAA National Centers for Environmental Information. (2001). *Global surface hourly (USW00054795; NH Durham 2 SSW)*. NOAA National Centers for Environmental Information.

NOAA's Coastal Change Analysis Program (C-CAP). (2016). Regional land cover data—coastal United States. Office for Coastal Management (OCM). Retrieved from www.fisheries.noaa.gov/inport/item/48336

Perez-Rodriguez, M., & Biester, H. (2022). Sensitivity of river catchments to discharge-controlled dissolved carbon export: A study of eight catchments in southern Patagonia. *Biogeochemistry*, *106*(2), 177–197. https://doi.org/10.1007/s10533-022-00947-3

Potter, J. D., Koenig, L., McDowell, W. H., & Snyder, L. (2020). *New Hampshire EPSCoR intensive aquatic network continuous discharge, nitrate, fDOM, temperature, and specific conductance data*. HydroShare. https://doi.org/10.4211/hs.8217eab0997d493782ff321ca5f95f28

Preston, S. D., Bierman, V. J., Jr., & Silliman, S. E. (1989). An evaluation of methods for the estimation of tributary mass loads. *Water Resources Research*, *25*(6), 1379–1389. https://doi.org/10.1029/WR025i006p01379

Radolinski, J., Le, H., Hilaire, S. S., Xia, K., Scott, D., & Stewart, R. D. (2022). A spectrum of preferential flow alters solute mobility in soils. *Scientific Reports*, *12*(1), 4261. https://doi.org/10.1038/s41598-022-08241-w

Rose, L. A., Karwan, D. L., & Godsey, S. E. (2018). Concentration–discharge relationships describe solute and sediment mobilization, reaction, and transport at event and longer timescales. *Hydrological Processes*, *32*(18), 2829–2844. https://doi.org/10.1002/hyp.13235

Seibert, J., Grabs, T., Köhler, S., Laudon, H., Winterdahl, M., & Bishop, K. (2009). Linking soil-and stream-water chemistry based on a riparian flow-concentration integration model. *Hydrology and Earth System Sciences*, *13*(12), 2287–2297. https://doi.org/10.5194/hess-13-2287-2009

Shattuck, M. D., Fazekas, H. M., Wymore, A. S., Cox, A., & McDowell, W. H. (2023). Salinization of stream water and groundwater at daily to decadal scales in a temperate climate. *Limnology and Oceanography Letters*, *8*(1), 131–140. https://doi.org/10.1002/lol2.10306

Sheldon, W. (2015). GCE data toolbox for MATLAB—public version 3.93. Georgia Coastal Ecosystems LTER File Archive website Retrieved from http://gce-lter.marsci.uga.edu/public/app/resource_details.asp?id5356

Silge, J., Chow, F., Kuhn, M., & Wickham, H. (2021). *Rsample: General resampling infrastructure*. General Resampling Infrastructure.

Šimůnek, J., Jarvis, N. J., van Genuchten, M. T., & Gärdenäs, A. (2003). Review and comparison of model for describing non-equilibrium and preferential flow and transport in the vadose zone. *Journal of Hydrology*, *272*(1–4), 14–35. https://doi.org/10.1016/S0022-1694(02)00252-4

Snyder, L., Potter, J. D., & McDowell, W. H. (2017). An evaluation of nitrate, fDOM, and turbidity sensors in New Hampshire streams. *Water Resources Research*, *54*(3), 2466–2479. https://doi.org/10.1002/2017WR020678

Snyder, W. M. (1969). Comments on "base-flow recessions – A review" by Francis R. Hall. *Water Resources Research*, *5*(4), 912–913. https://doi.org/10.1029/wr005i004p00912

Speir, S. L., Tank, J. L., Bieroza, M., Mahl, U. H., & Royer, T. V. (2021). Storm size and hydrologic modification influence nitrate mobilization and transport in agricultural watersheds. *Biogeochemistry*, *156*(3), 319–334. https://doi.org/10.1007/s10533-021-00847-y

Sujono, J., Shikasho, S., & Hiramatsu, K. (2004). A comparison of techniques for hydrograph recession analysis. *Hydrological Processes*, *18*(3), 403–413. https://doi.org/10.1002/hyp.1247

Tashie, A., Pavelsky, T., & Band, L. E. (2020). An empirical reevaluation of streamflow recession analysis at the continental scale. *Water Resources Research*, *56*(1), e2019WR025448. https://doi.org/10.1029/2019WR025448

Teuling, A. J., Lehner, I., Kirchner, J. W., & Seneviratne, S. I. (2010). Catchments as simple dynamical systems: Experience from a Swiss prealpine catchment. *Water Resources Research*, *46*(10). https://doi.org/10.1029/2009WR008777

Torres, M. A., & Baronas, J. J. (2021). Modulation of riverine concentration-discharge relationships by changes in the shape of the water transit time distribution. *Global Biogeochemical Cycles*, *35*(1), e2020GB006694. https://doi.org/10.1029/2020GB006694

Tunqui Neira, J. M., Andréassian, V., Tallec, G., & Mouchel, J. M. (2020). A two-sided affine power scaling relationship to represent the concentration–discharge relationship. *Hydrology and Earth System Sciences*, *24*(4), 1823–1830. https://doi.org/10.5194/hess-24-1823-2020

Tunqui Neira, J. M., Andréassian, V., Tallec, G., & Mouchel, J. M. (2021). Multi-objective fitting of concentration-discharge relationships. *Hydrological Processes*, *35*(11), e14428. https://doi.org/10.1002/hyp.14428

Underwood, K. L., Rizzo, D. M., Schroth, A. W., & Dewoolkar, M. M. (2017). Evaluating spatial variability in sediment and phosphorus concentration-discharge relationships using Bayesian inference and self-organizing maps. *Water Resources Research*, *53*(12), 10293–10316. https://doi.org/10.1002/2017WR021353

Vaughan, M. C. H., Bowden, W. B., Shanley, J. B., Vermilyea, A., Sleeper, R., Gold, A. J., et al. (2017). High-frequency dissolved organic carbon and nitrate measurements reveal differences in storm hysteresis and loading in relation to land cover and seasonality. *Water Resources Research*, *53*(7), 5345–5363. https://doi.org/10.1002/2017WR020491

Walling, D. E. (1975). *Solute variations in small catchment streams: Some comments* (Vol. 64, pp. 141–147). The Royal Geography Society (with the institute of British Geographers). https://doi.org/10.2307/621472

Wickham, H., François, R., Henry, L., & Müller, K. (2021). Package dplyr. Version 1.0. 7.

Wymore, A. S., Brereton, R. L., Ibarra, D., Maher, K., & McDowell, W. H. (2017). Critical zone structure controls concentration-runoff relationships in watersheds draining a tropical montane forest. *Water Resources Research*, *53*(7), 6279–6295. https://doi.org/10.1002/2016WR020016

Wymore, A. S., Leon, M. C., Shanley, J. B., & McDowell, W. H. (2019). Hysteretic response of solutes and turbidity at the event scale across forested tropical montane watersheds. *Frontiers in Earth Science*, *7*. https://doi.org/10.3389/feart.2019.00126

Wymore, A. S., Shattuck, M. D., Potter, J. D., Snyder, L., & McDowell, W. H. (2021). The Lamprey River Hydrological observatory: Suburbanization and changing seasonality. *Hydrological Processes*, *35*(4). https://doi.org/10.1002/hyp.14131

Zarnetske, J. P., Bouda, M., Abbott, B. W., Saiers, J., & Raymond, P. A. (2018). Generality of hydrologic transport limitation of watershed organic carbon flux across ecoregions of the United States. *Geophysical Research Letters*, *45*(21), 702–711. https://doi.org/10.1029/2018GL080005

Zimmer, M. A., Pellerin, B., Burns, D. A., & Petrochenkov, G. (2019). Temporal variability in nitrate-discharge relationships in large rivers as revealed by high-frequency data. *Water Resources Research*, *55*(2), 973–989. https://doi.org/10.1029/2018WR023478